The Behaviours of Various DC Choppers during Shading Occurrence in PV Systems

SAMEER KHADER, ABDEL-KARIM DAUD
Department of Electrical Engineering,
Palestine Polytechnic University (PPU),
P.O. Box 198, Hebron,
PALESTINE

Abstract: - This paper investigates how the DC choppers behave during the shading occurrence at different time intervals of the year. Three types of DC choppers are implemented during the same shading conditions and intervals of time. The studied parameters are the duty cycle, output power, current, and switch losses. The mathematical model is built and implemented using the MATLAB/Simulink platform. The obtained results show that the SEPIC converter has the highest rate of duty cycle, which means more switching losses are generated. Concerning the average output power, the Modified Single Ended Primary Converter (MSEPIC) has the highest rate, while the Boost Converter has the lowest rate. The MPP power, duty cycle, and switching losses are studied under various shading rates. The duty cycle has the highest rate on the SEPIC converter, while MSEPIC has the lowest rate. Despite that, the switching losses are tremendously high at MSEPIC compared to SEPIC converters. Furthermore, simulation studies show that Boost and SEPIC converters have better performance in frequent cloudy weather conditions.

Key-Words: - Modified SEPIC Converter, PID Controller, Photovoltaic Source, PWM, MPPT, Modelling, Partial Shading.

Received: August 23, 2023. Revised: February 16, 2024. Accepted: March 14, 2024. Published: April 22, 2024.

1 Introduction

As well-known renewable energy (RE) resources found widespread utilization throughout the whole world, aiming at reducing the dependency on fossil oil sources, and reducing the negative impact of conventional energy sources on the environment, [1], [2]. One of the most important RE resources is the photovoltaic (PV) solar energy source, which has a sustainable status and is friendly to the environment, [3], [4]. The mentioned PV source depends on the sun location during the year and has a variable irradiation rate with an average value of about 5.3 kWh/m^2 per day for Palestine, which is located at a latitude of 31.58°N and a longitude angle of 35.14°E. Usually, the PV system consists of several power generation, conversion, and control units that are the core of the system. Shadowing is one of the most important factors that causes a significant reduction in generated energy, [5], [6]. Taking into account the approach of [7], direct detection of the maximum power at any value of solar irradiation and temperature during the daytime is realized. Various DC-DC converters are applied, such as the single and modified single-ended primary-inductance converters SEPIC and MSEPIC, respectively, in addition to the well-known boost converter, [8], [9]. Figure 1(a) illustrates the principal electrical circuit for MSEPIC, while Figure 1(b) presents the control circuit with a partial shading condition. The proposed model is analyzed and simulated in MATLAB/ Simulink, and m-file code, [10]. Closed-loop feedback control with a PID controller based on a triggering system is developed for the MSEPIC converter to maintain a constant output voltage, as shown in Figure 1(b).

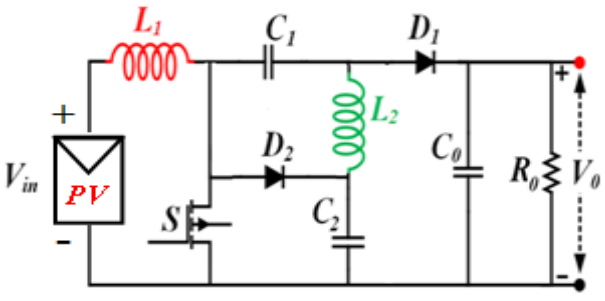

a) Principle electrical circuit

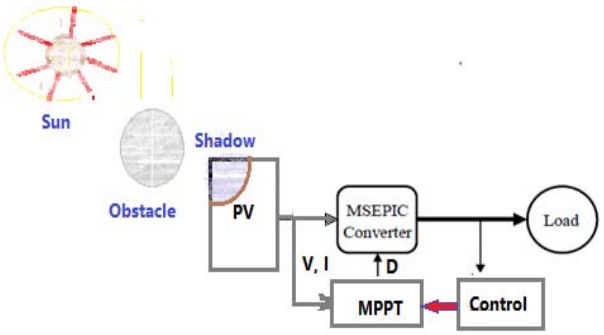

b) Control circuit

Fig. 1: Modified SEPIC Converter, [11]

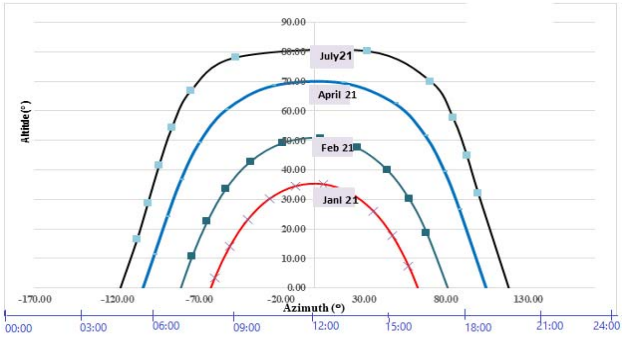

Fig. 2: Plot of solar altitude versus azimuth for different months of the year at a latitude of 31.58 N, [12]

2 Mathematical Modelling

2.1 The Sun Path for Palestine

Depending on the sun's position, the position of the PV panel, and surrounding objects, partial or complete shading can occur. The sun position is defined as a function of the daytime, latitude, and longitude in order to determine the shaded area of the PV panel. According to [13], [14], the solar equations are implemented in the Excel platform, [15], for Palestinian city of Hebron, which is located at a latitude of 31.58°N and a longitude angle of 35.14°E. The plots of altitude versus azimuth angles are displayed in Figure 2, where it is clearly shown that the existence of hard shadow such as trees or solid obstacles severely affects the winter months rather than the summer months.

2.2 The Effect of Shading on Circuit Parameters

When solar irradiation intensity varies during the day, it causes a significant change in the extracted power in terms of voltage and current at a given temperature. This variation can occur due to soft and hard shading factors, such as cloudy weather that causes soft shading and trees or buildings that cause hard shading. The significant variation occurs in the generated current while there is a light change in the voltage. To estimate the effect of shading on the PV system parameters, the PV voltage and current are derived as follows, [11], [12] and shown in Figure 3.

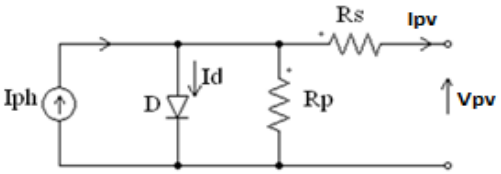

Fig. 3: Equivalent circuit for PV cell

The cell voltage at standard test conditions is:

$$V_{pv} = \frac{A\,K\,T_c}{q} \ln\left(\frac{I_{ph}+I_d-I_{pv}}{I_{pv}}\right) - R_s\,I_{pv} \quad (1)$$

where A is the diode idealistic factor, I_d is the diode saturation current, I_{ph} is the cell photo current, I_{PV} is the photovoltaic current, K is the Boltzmann constant, q is the electric charge, and R_s is the PV series resistance. While the photocurrent in terms of irradiation and temperature is:

$$I_{ph} = N_p \left[I_{sc}\, {}^{G}/_{G_r} + I_t(T_c - T_r) \right] \quad (2)$$

where G_r is the reference solar irradiation and I_{SC} is the short circuit current.

The output cell current is:

$$I_{pv} = N_p \left[I_{ph} - I_d \left(\exp\left(\frac{q\, {}^{V_0}/_{N_s}}{A\,K\,T_c} \right) - 1 \right) \right] \quad (3)$$

The diode current can be stated as:

$$I_d = I_{or} \left(\frac{T_c}{T_r}\right)^3 exp\left[\left(\frac{q\,E_g}{B\,K}\right)\left(\frac{1}{T_r} - \frac{1}{T_c}\right) \right] \quad (4)$$

where B is the diode idealistic factor, E_g is the band gap energy of the semiconductor, T_c and T_r are the cell and reference temperature, respectively, and I_{or} is a constant given at standard conditions. The idealistic diode factors A and B have values that vary between 1 and 2 depending on I-V performance shaping and approximations.

2.3 Photovoltaic System in a SIMULINK Environment

A photovoltaic model is built on the MATLAB/Simulink platform without the shading effect, as shown in Figure 4 for the solar panel type SUNPOWER, SPR-315E, with a 315-watts peak and a conversion efficiency of 20.5% , [16]. To show the effect of shading on PV performances, three PV panels are connected in series with 0%, 33%, and 66% shading rates, as shown in Figure 5.

The obtained results are graphically presented in Figure 6, where it's clearly shown that the effect of shading causes a dramatic reduction in total PV power up to 53% of the total value, and concerning current, the reduction exceeds 22%. Furthermore, the overall performance deformation occurs when the MPPT algorithm detects less power with a reduced voltage that corresponds to the maximum power point. Figure 7 illustrates the time domain of solar variation, V_{mpp} and V_{out} for December 21st with a 15% shading rate, while Figure 8 and Figure 9 illustrate the 3D variation of solar irradiation, power and voltage at MPP during the previous mentioned day using a boost converter.

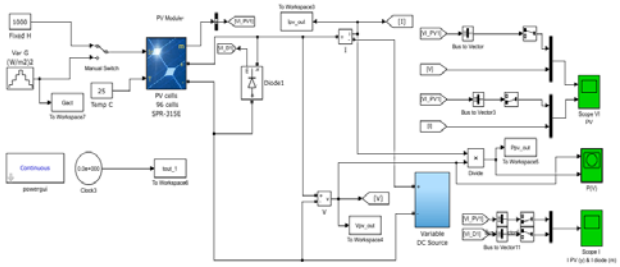

Fig. 4: Simulink model for a single PV array with no shading effect

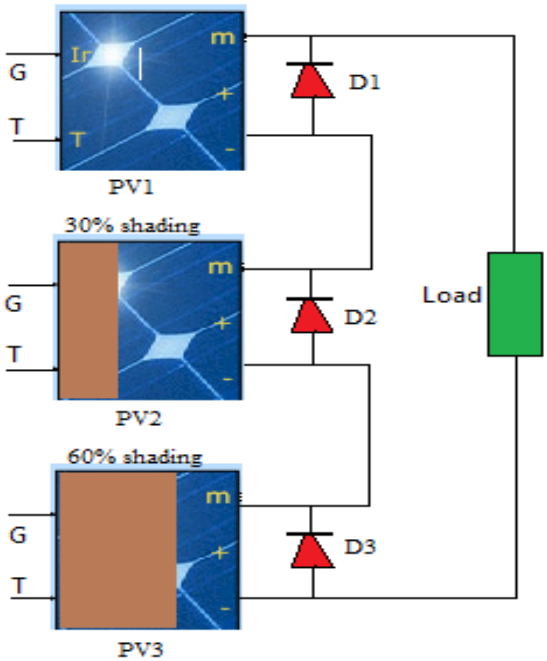

Fig. 5: PV panels with various shading rate

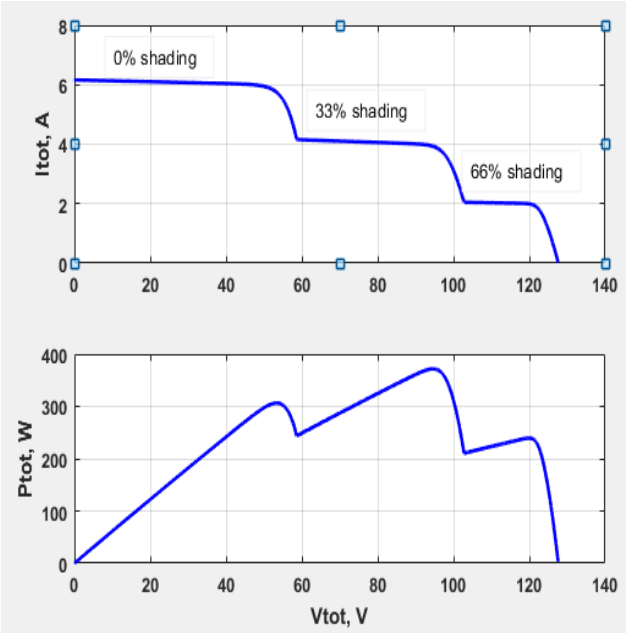

Fig. 6: PV performances for SPR-315E at STC

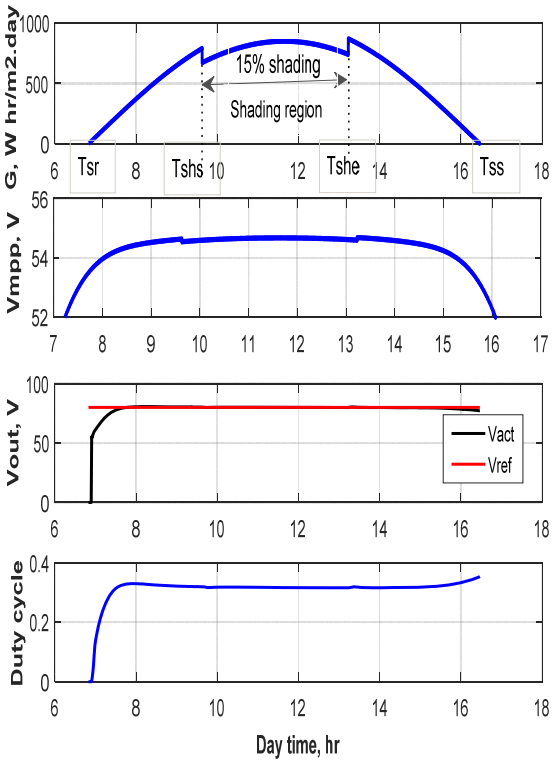

Fig. 7: Solar and voltage variation during December 21st with 15% shading

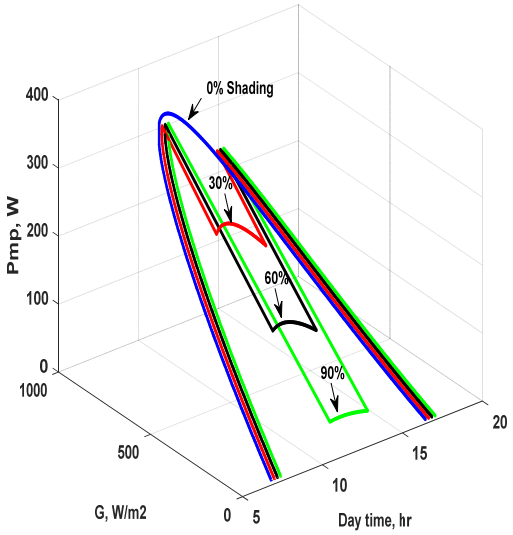

Fig. 8: Power at MPP for SPR-315E at various shading rate

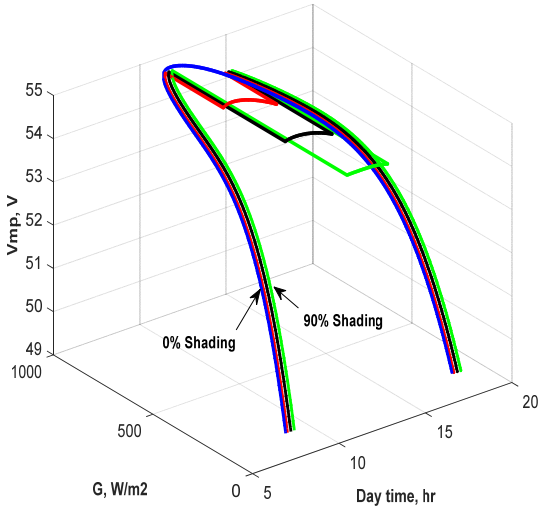

Fig. 9: Voltage at MPP for SPR-315E at various shading rates

3 Shading and Converters

As previously mentioned, three converter types are simulated under the same shading conditions and rated temperature of 25°C with data given in Table 1. The following simulation results can be discussed as follows:

3.1 The Average Irradiation

To estimate the effect of shadow rate on the main PV and load parameters, it is necessary to determine the average value of solar irradiation. Referring to Figure 7, where the shadow region is illustrated, the average daily irradiation can be presented according to eq. (5):

$$G_{avg} = \frac{G_{max}}{T_d}\left[\int_{T_{sr}}^{T_{ss}} \sin(t - T_{sr})dt - K_{sh}\int_{T_{shs}}^{T_{she}} \sin(t - T_{sr})dt\right];$$

with

$$Gavg\% = \frac{G_{avg}}{Gmax}.100 \quad (5)$$

where T_d is the day duration, [17], T_{sr} and T_{ss} are the sunrise and sunset respectively, G_{max} is the maximum irradiation at full sun, T_{shs} and T_{she} are the start and end times of the shadow, respectively, and K_{sh} is the shadow rate that varies in the range of 0% to 90%, [17], [18], [19], [20].

Solving eq. (5) for certain days of the year and at fixed start and end shadow times (T_{shs}=9:30, T_{she}=13:30) AM and varying the shadow rate yields Figure 10(a) where the average value drops from 65% to 43%. While Figure 10(b), shows the average values of voltage at MPP as the shadow rate increases.

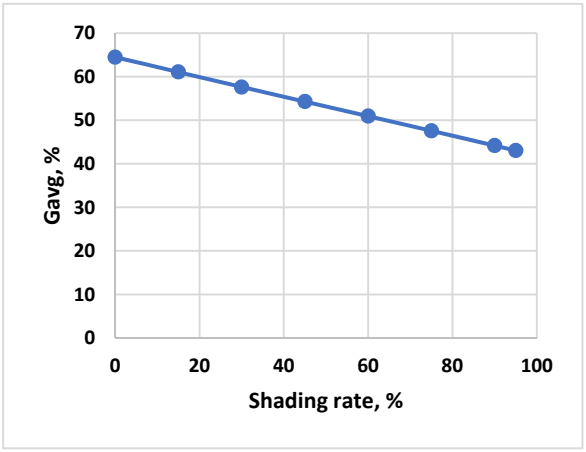

a) Average irradiation

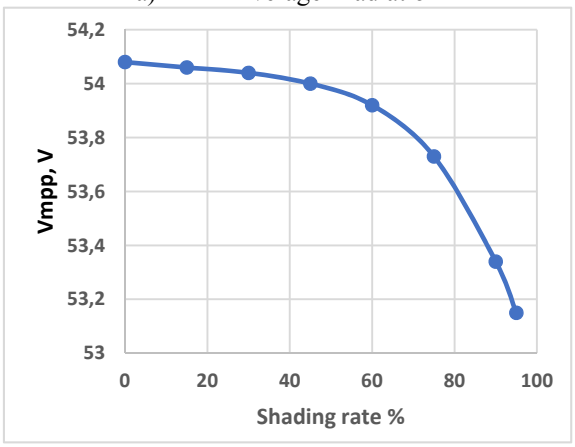

b) Average voltage at MPP

Fig. 10: Solar irradiation, voltage and power at December 21st

3.2 The Variation of Duty Cycle and Output Voltage

The duty cycle depends on the chopper type, input, and output voltage at a given solar irradiation. The duty cycle can be expressed according to eq. (6):

$$D_{BOOST} = \frac{V_{Load} - V_{mpp}}{V_{Load}}$$

$$D_{SEPIC} = \frac{V_{Load}}{V_{Load}+V_{mpp}} \quad (6)$$

$$D_{MSEPIC} = \frac{V_{Load} - V_{mpp}}{V_{Load} + V_{mpp}}$$

where V_{Load} is the load voltage and V_{mpp} is the voltage at MPP and given irradiation.

Figure 11 illustrates the change of duty cycle for various converter types, and the shading rate varies from 0% to 90%. It can be shown that the variation of V_{mpp} is negligible among the entire shading rates, as shown in Figure 10(b), where the voltage varies in the range of 54.2V to about 52V as the shadow rate changes from 0% to 90%.

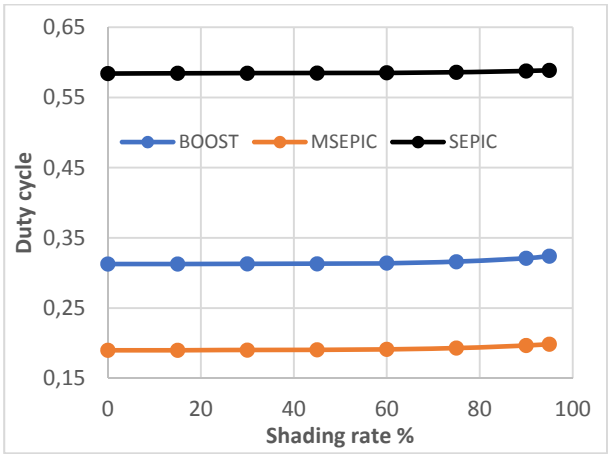

Fig. 11: Duty cycle at variable shading rate

The percentage load voltage variation with respect to the reference voltage and various shading rates can be estimated according to eq. (7).

$$\Delta V\% = \frac{V_{ref} - V_{Load}}{V_{ref}} * 100 \quad (7)$$

where V_{ref}=80V is the stated reference load voltage and V_{Load} is the actual load voltage obtained at various chopper types.

Figure 12 shows that the SEPIC converter has the largest voltage change with respect to the reference, while the MSEPIC converter has the least voltage change, which is around 0.9%, converted to a physical value of V_{ref}=80V and V_{Load}=79.28V.

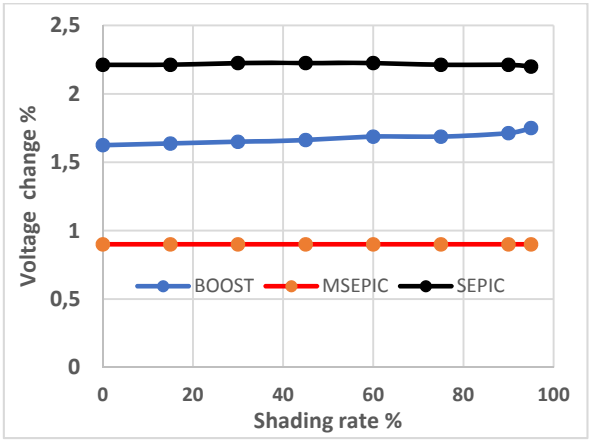

Fig. 12: Percentage change of load voltage

3.3 The Variation of Load Power and Efficiency

As the shading rate increases, the load power decreases as well, while the chopper losses slightly increase due to the observed change in the duty cycle. According to [4], the daily lost power due to continuous transistor switching aimed at operating at MPP can be presented as follows:

$$P_{QAV}(T_{day}) = \frac{Kq}{T_{day}} \int_{t_{SR}}^{tss} P_{QD}(n_1)dt$$

$$= a_{g2}\left(\frac{Am^2}{2} - \frac{4\,Am\,Bm}{\pi} + Bm^2\right) + \quad (8)$$

$$+ a_{g1}\left(\frac{2Am}{\pi} + Bm\right) + a_{g0}$$

where T_{day} is the day duration; n_1 is the day number (n_1=1..365); $Am = G_{max}/250$, $Bm = 2.4$, and Kq=1.12 is the correction factor; a_{g2} = -0.066, a_{g1} = 0.062, and a_{g0} = 0.78.

P_{QD} is the dissipated power of the transistor switch that can be expressed according to eq. (9) in terms of solar irradiation.

$$P_{QD}(G) = a_{g6}Z^6 + a_{g5}Z^5 + a_{g4}Z^4 + a_{g3}Z^3 + \\ + a_{g2}Z^2 + a_{g1}Z + a_{g0} \quad (9)$$

where
a_{g6} = -0.0083, a_{g5}= 0.01, a_{g4} = 0.04, a_{g3}=-0.043, a_{g2}= -0.066, a_{g0} = 0.78,

and

$$Z = \frac{\left[\left(G_{max}\sin\left(\frac{\pi}{T}(t - t_{SR})\right) - 600\right]\right.}{250}$$

The observed transistor energy loss in terms of heat for both described chopper types is illustrated in Figure 13. It can be noticed that due to the large value of the duty cycle of the SEPIC converter, the transistor losses have larger values compared to the BOOST converter. The output average power can be presented according to eq. (10):

$$P_{out} = P_{pv\_avg} - P_{QD\_avg}$$

and $$\eta_{\%} = \frac{P_{out}}{P_{pv\_avg}} * 100 \quad (10)$$

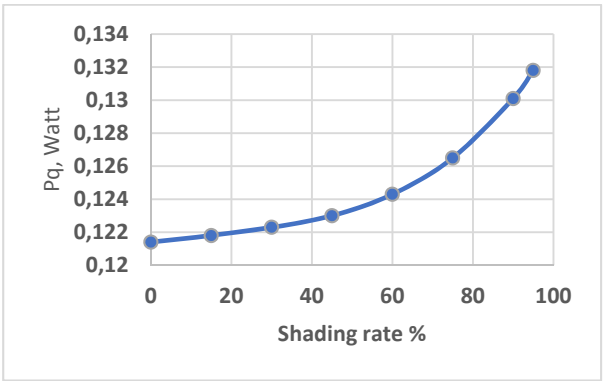

a) Boost converter

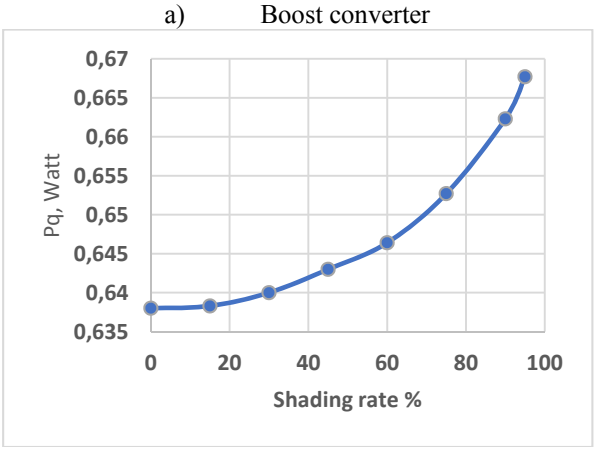

b) SEPIC converter

Fig. 13: IGBT transistor loss at various shading

The obtained simulation results according to eq. (10) are displayed in Figure 14 for three converter types. As well as shown in Figure 14(a), increasing the shading rate heavily affects the load power; furthermore, BOOST and SEPIC converters have identical changes, while MSEPIC is affected due to shading. Figure 14(b) confirmed that the efficiency of the MSEPIC converter reduces as the shadow rate increases, while other converters have, to some extent, unaffected efficiency. Which means MSEPIC converter presents an inefficient solution in areas with frequent shading status.

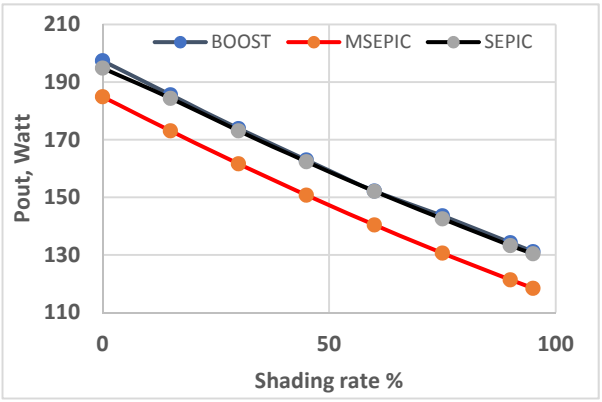

a) Average output power

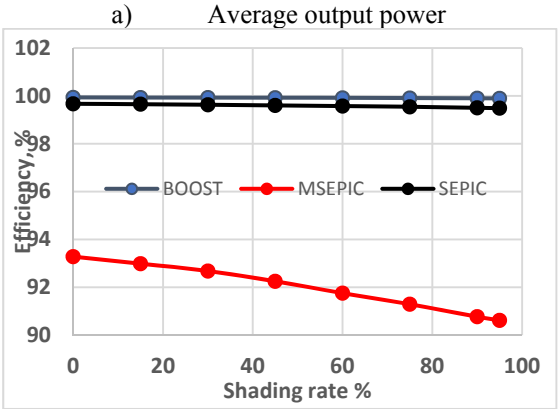

b) Average efficiency

Fig. 14: Output power and efficiency on December 21st

3.4 The Most Affected Month of Shadowing

To see which months are most affected by shading, the average irradiation rate is calculated at the same shading conditions of 60% and the same shading start and end duration for all twelve months at the 21st of the month. The result is illustrated in Figure 15 according to eq. (11).

$$G_{AV\_M}\% = \frac{G_{USH} - G_{SH}}{G_{USH}} 100 \quad (11)$$

where G_{USH}= 636.67 Wh/m^2-day is the average irradiation in June 21st which is the longest day of the year, and G_{SH} is the average irradiation under shading conditions for a given month.

It can be shown that the winter months are the most affected by the shadow, with irradiation reduction up to 20% at a 60% shading rate.

Table 1. Data specification for SPR-315E-WHT-D

q	K	I_{ph}	I_d	R_S	R_P
1.602e-19 C	1.38e-23J/°K	6.14A	0.059A	0.15Ω	1090Ω
N_S	N_P	V_{cell}	V_{OC}	I_{SC}	V_{MPP}
32	3	0.6V	64.6V	6.14A	54.7V
I_{MPP}	P_{MPP}	Eg	N_{Pm}	V_{pv}	R_{load}
5.76A	312 W	1.1	1	54.7V	9.6Ω
Vin, V	Vo, V	D	L1, mH	L2, mH	C1, µF
Variable	Variable	0.1 – 0.9	1.98	0.99	660
C2, µF	Co, µF	Ro, Ω	T_C		
660	10	9.5	25°C		

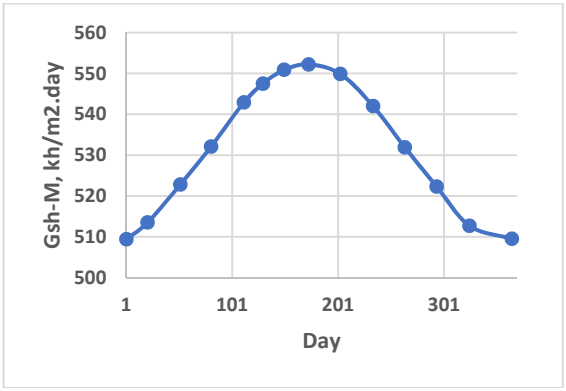

a) Average irradiation at 60% shading rate

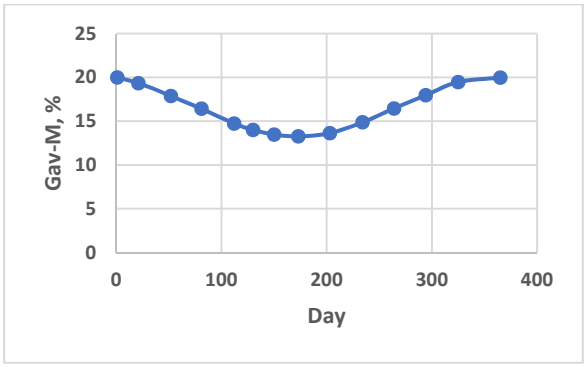

b) The percentage changes

Fig. 15: Average irradiation at 21st of the month

4 Conclusion

Taking into account the obtained simulation data at various chopper configurations, shading levels, and shading time intervals, the following conclusions can be drawn:

- The shading effect linearly affects the MPP current, while this effect has a nonlinear effect on the MPP voltage.
- Concerning the output or load power, MSEPIC converts less power compared to other chopper configurations. Furthermore, the chopper losses are tremendously high in MSEPIC compared to other converters.
- The winter months are the most affected by the shading condition, where the average irradiation falls by 20% when shading has a 60% effect?
- Therefore, it's recommended that Boost and SEPIC be most effective during shading conditions. This means installing MSEPIC converters must be avoided in frequent shading conditions. The same recommendation is valid for regions with a long winter season.

References:

[1] Martin, S. S., Chebak, A., Barka, N., Development of renewable energy laboratory based on integration of wind, solar and biodiesel energies through a virtual and physical environment, 2015, *3rd International Renewable and Sustainable Energy Conference, Marrakech, 2015*, pp. 1-8. https://doi.org/10.1109/irsec.2015.7455086.

[2] Mahmoud, Y., Xiao, W., Zeineldin, H. H., A simple approach to modeling and simulation of photovoltaic modules, *IEEE Trans. Sustain. Energy*, vol. 3, no. 1, Jan. 2012, pp. 185–186. https://doi.org/10.1109/tste.2011.2170776.

[3] Mastromauro, R. A., Liserre, M., Dell'Aquila, A., Control issues in single-stage photovoltaic systems: MPPT, current and voltage control, *IEEE Trans. Ind. Informat.*, vol. 8, no. 2, May. 2012, pp. 241– 254. https://doi.org/10.1109/tii.2012.2186973.

[4] Khader, S., Daud, A.K., Boost chopper behaviors in Solar photovoltaic system, *Smart Grid and Renewable Energy* , Vol.12, No.3, March 2021, pp. 31-52. https://doi.org/10.4236/sgre.2021.123003.

[5] Martín Silva, Justo Jose Roberts& Pedro Osvaldo Prado, " Calculation of the Shading Factors for Solar Modules with MATLAB", Energies 2021, 14(15), 4713; pp.1-23, https://doi.org/10.3390/en14154713.

[6] Rusiana Iskandar , Yuda Bakti Zainal, and Susanto Sambasr, "Study and Analysis of Shading Effects on Photovoltaic Application System", MATEC Web of Conferences Volume 218, ICIEE,2018, Indonesia. ,https://doi.org/10.1051/matecconf/201821802004

[7] Ammaiyappan, B. S., Seyezhai, R., Comparative analysis of Maximum Power Point Tracking Algorithms for Photovoltaic Applications, *WSEAS Transactions on Power Systems*, Vol. 15, 2020, pp.161- 171, https://doi.org/10.37394/232016.2020.15.20.

[8] Hasan J., Ferjana S., Chowdhury S., "Investigation of Power Performance of a PV Module with Boost Converter Using MATLAB Simulation", *American International Journal of Sciences and Engineering Research*, pp.1-13, June, 29, 2021, https://doi.org/10.46545/aijser.v4i1.322

[9] Daud, A.K., Khader. S.H., Closed Loop Modified SEPIC Converter for Photovoltaic System, *WSEAS Transaction on Circuits and Systems*, Vol. 21, pp161-167, 2022, https://doi.org/10.37394/23201.2022.21.17.

[10] MATLAB and Simulink (2016) The MathWorks, Inc., version R2016b, [Online]. http://www.mathworks.com (Accessed Date: April 13, 2024).

[11] Omeje Crescent Onyebuchi," Power loss analysis model of a dc-dc buck-boost converter with an interfaced three phase inverter for medium voltage application ", *Journal of Asian Scientific Research*, ISSN(e): 2223-1331 , Vol. 9, No. 8, 100-115, 2019, https://doi.org/10.18488/journal.2.2019.98.100.115.

[12] Lydeni, S., Haque, M. E., "Modelling, parameter estimation and assessment of partial shading conditions of photovoltaic modules", *J. Mod. Power Syst. Clean Energy*, 2018, https://doi.org/10.1007/s40565-018-0454-9.

[13] Numan, A.H.; Dawood, Z.S.; Hussein, H.A. Theoretical and experimental analysis of photovoltaic module characteristics under different partial shading conditions. *Int. J. Power Electron. Drive Syst.* 2020, 11, 1508–1518, http://doi.org/10.11591/ijpeds.v11.i3.pp1508-1518.

[14] Kazem H.A., Chaichan M.T., Alwaeli A.H, Mani K., Effect of shadows on the performance of solar photovoltaic, *Mediterranean Green Buildings & Renewable Energy*. Springer, Cham, https://doi.org/10.1007/978-3-319-30746-6_27.

[15] Wang, Y., Yang, B., "Optimal PV array reconfiguration under partial shading condition through dynamic leader based collective intelligence", *Protection and Control of Modern Power Systems*, Vol. 8, Article number: 40 (2023), 16 pages, https://doi.org/10.1186/s41601-023-00315-9.

[16] SUNPOWER PV Datasheet, SPR-315E (8), [Online]. https://www.solarfeeds.com/product/spr-p3-315-335-blk/

[17] Gilbert M. Masters, *Renewable and Efficient Electric Power Systems,* 2nd Edition, Ch4, pp. 186-247, ISBN-13: 978-1118140628, 2017, [Online]. http://www.a-ghadimi.com/files/Courses/Renewable%20Energy/REN_Book.pdf (Accessed Date: April 13, 2024).

[18] Quaschning, V., Hanitsch, R. Shade Calculations in Photovoltaic Systems. *In Proceedings of the ISES Solar World Conference*, Harare, Zimbabwe, 11–15 September 1995, [Online]. https://www.volker-quaschning.de/downloads/ ISES1995.pdf

[19] MacAlpine, S., Deline, C., Dobos, A., "Measured and Estimated Performance of a Fleet of Shaded Photovoltaic Systems with String-and-Module-Level Inverters", *Progress in Photovoltaics Research and Applications*, March 2017, Vol. 25, Issue 8, p. 714-726, DOI: 10.1002/pip.2884

[20] Nahidan, M. H., Niroomand, M., Dehkordi, B.M., "Power Enhancement under Partial Shading Condition Using a Two-Step Optimal PV Array Reconfiguration", *International Journal of Photoenergy*, Vol. 2021, January 2021, 19 pages, https://doi.org/10.1155/2021/8811149.

Contribution of Individual Authors to the Creation of a Scientific Article (Ghostwriting Policy)

- Sameer Khader implemented the SIMULINK model and presented building performances, conclusions, and paper preparation.
- Abdel-Karim Daud has performed the literature review, carried out the mathematical model, analyzed the numerical results, discussed the results, drawn a conclusion, and finalized the paper.

Sources of Funding for Research Presented in a Scientific Article or Scientific Article Itself

No funding was received for conducting this study.

Conflict of Interest

The authors have no conflicts of interest to declare.